Tribol Lett
DOI 10.1007/s11249-013-0271-2

ORIGINAL PAPER

Evolution in Surfaces: Interaction of Topography with Contact Pressure During Wear of Composites Including Dinosaur Dentition

Kyle G. Rowe · Gregory M. Erickson · W. Gregory Sawyer · Brandon A. Krick

Received: 27 September 2013 / Accepted: 21 November 2013

Abstract A two-parameter elastic foundation model is used to predict the coupled evolution of contact pressure and wear of multicomponent composite surfaces. The iterative model predicts the evolution of surface shape for an initially flat multicomponent surface under uniform applied pressure; where the components of the composite surface are different materials of different wear rates. The model is applied to elucidate the chewing surface morphology of the dentition in a hadrosaurid dinosaur using wear rates measured from fossilized dental tissues. Additionally, to further illustrate the predictive capabilities of the coupled contact pressure and wear model, a two-component polymer sample was fabricated and experimentally evaluated through laboratory wear experiments. Data obtained from the abrasive wear testing of a laboratory multicomponent polymer sample was compared to model predictions using measured system and material parameters. Differences between the measured and predicted surface profiles were on the same order as the sample's surface roughness (Ra $\sim$3 μm).

Keywords Wear · Dental wear · Dinosaur · Wear modeling · Contact pressure

K. G. Rowe · W. G. Sawyer
Department of Mechanical and Aerospace Engineering, University of Florida, Gainesville, FL 32611, USA

G. M. Erickson
Department of Biological Science, Florida State University, Tallahassee, FL 32306-4295, USA

B. A. Krick (✉)
Department of Mechanical Engineering and Mechanics, Lehigh University, Bethlehem, PA 18015, USA
e-mail: bakrick@lehigh.edu

1 Introduction

As the demand for low-wear materials grows so does the need for accurate, fast, and efficient wear predictions. These predictions are useful for estimating component or device service life and can be used as a component of mechanical design. A great deal of attention has been given to predicting the topological evolution of a wearing surface; the results of which are of practical importance to numerous systems and applications.

Of the varied approaches to the problem of wear prediction, closed-form solutions are in the minority. The few that do exist are for simple mechanisms such as the scotch-yolk, cylindrical bushings, and eccentrically mounted cam-follower systems [1–4]. Due to the mechanical complexity of most systems and the continuously evolving contact conditions created by wear, numerical, and finite elemental method (FEM), approaches are more frequently applied to such problems [5–14]. In these simulations, contact pressure calculations must be made at each time step. This has the potential to be computationally expensive, making it desirable to have a fast and efficient method for computing local pressures while incorporating relevant information about evolved surface geometries. The added complexities of multi-material systems that contain constituents with different tribological properties are of most interest in this paper.

In this manuscript, a two-dimensional model, previously proposed by Sawyer [15] for the evolution of contact pressure and wear of a two-component surface, is extended to three-dimensional multicomponent surfaces. It predicts the evolution of surface shape for an initially flat composite surface of multiple materials, each with a different wear rate, using a two-parameter elastic foundation model for contact pressure calculations. The two-dimensional model was previously used to explain surface phenomena

Published online: 07 December 2013

associated with copper chemical mechanical polishing [15] and in a recent report, a three-dimensional adaptation of the model was used to elucidate tissue-level contributions to dental form and function in fossilized dinosaurian dental batteries [16]. Details of the models' application to dinosaur dentition will be discussed.

Additionally, the three-dimensional model is presented and applied to the wear evolution of a two-component laboratory sample consisting of polyetheretherketone (PEEK) and epoxy. In an attempt to demonstrate capabilities of the model, the idealized system was constructed and tested under abrasive wearing conditions, where all modeling input parameters were either known or measured. Results from laboratory experiments are compared with model predictions.

2 Modeling

A two-parameter elastic foundation model, based on the pressure–displacement relationship given by Eq. 1, was used to incorporate the combined effects of gross pad deflection and curvature on the foundation reaction pressure in three dimensions [15, 17]. Here, P is the local foundation reaction pressure, z is the local deflection of the foundation, K_s is the first foundation parameter, and K_g is the second foundation parameter. The deflection of the pad under a uniform applied pressure, P_0, is given by Eq. 2. A model of the problem is illustrated in Fig. 1a.

$$p = k_s z - k_g \left(\frac{d^2 z}{dx^2} + \frac{d^2 z}{dy^2} \right) \tag{1}$$

$$z_0 = \frac{P_0}{k_s} \tag{2}$$

Gross pad deflection is well estimated by the Winkler foundation model when dealing with planar surfaces. However, the model assumes there is no coupling between neighboring elements of the pad. Therefore, the second term, akin to a plate lying on a bed of springs [18], is used in the analysis to recover surface curvature. The Winkler model alone would either over or under predict contact pressures depending on the curvature direction, but by incorporating both terms in the analysis, it is possible to predict the evolution from planar to nonplanar surface geometries using basic mechanics.

The incremental wear depth, Δh (mm) at a particular location is calculated using Eq. 3, where Δs (mm) is an incremental slip distance and K (mm^3/Nm) is a material wear rate. Most wear models may be cast in the form of Eq. 3 and as such may be used with discretion.

$$\Delta h = \frac{p \Delta s}{K} \tag{3}$$

Fig. 1 Coupled wear evolution model overview (**a**) illustrating the ▶ two-parameter elastic foundation model and unworn (*top*) and worn (*bottom*) multicomponent surfaces. The model is applicable to simple or very complex systems comprised of numerous materials each with distinct material properties. One example is the hadrosaurid dental battery (**b** *top view*) where the chewing surface morphology of the dinosaur was elucidated using measured wear data from fossilized dental tissues. A comprehensive overview of how wear evolves under a constant nominal pressure (**c**) is shown along with the final steady state surface (**d**)

The iterative solution procedure, previously outlined by Sawyer [15], uses a numerical approach where each surface element is assigned a specific wear resistance. Although in this investigation, material wear rates were assumed constant and the iterative nature of the solution can accommodate time, velocity, or pressure-dependent wear rates.

An example of this model's utility is given in Fig. 1b–d where it has been applied to the abrasive wear of the complex dental battery of a hadrosaurid dinosaur, a large herbivore with a duck-like bill and grinding dentition from the Late Cretaceous period [16]. In the *Science* report [16], it was revealed that the hardness and wear properties of hadrosaurid dental tissues could be recovered from the fossilized dental batteries. Mechanical and tribological properties had not been previously measured in fossil teeth; nevertheless, they should be preserved, since hydroxyapatite mineral content, not protein presence, is the primary contributor to the tissue hardness.

To characterize hadrosaurid dental tissue wear rates, we subjected teeth from an intact dental battery (AMNH 5896; American Museum of Natural History, New York, NY, USA) of *Edmontosaurus* (a taxon possessing all hadrosaurid dental tissues) to micro-tribological wear testing [16]. A diamond-tipped probe (analogous to abrasive grit) was reciprocated across the tooth at 1 mm/s with 100 mN normal force to mimic abrasive feeding strokes, and worn tissue volume was measured with an optical profiler to calculate wear rates [16]. Although one might expect multidirectional sliding to be more relevant, wear rates of tissues (some tissue regions smaller than a few 100 µm across) are most easily measured with this sharp probe on tissue in a single-direction linear reciprocating motion. Multiple reciprocating experiments were performed at angles relative to the feeding direction (parallel to the long axis of the median carina, one at 40° and another at −30°) with little variation in measured wear rates to eliminate directionality concerns. The ability to predict the complex multitiered morphology of the chewing surfaces using a wear simulation incorporating both the tissue distributions and their respective wear rates supports the theory that relative wear properties are preserved in the fossil teeth [16]; furthermore experiments comparing modern and

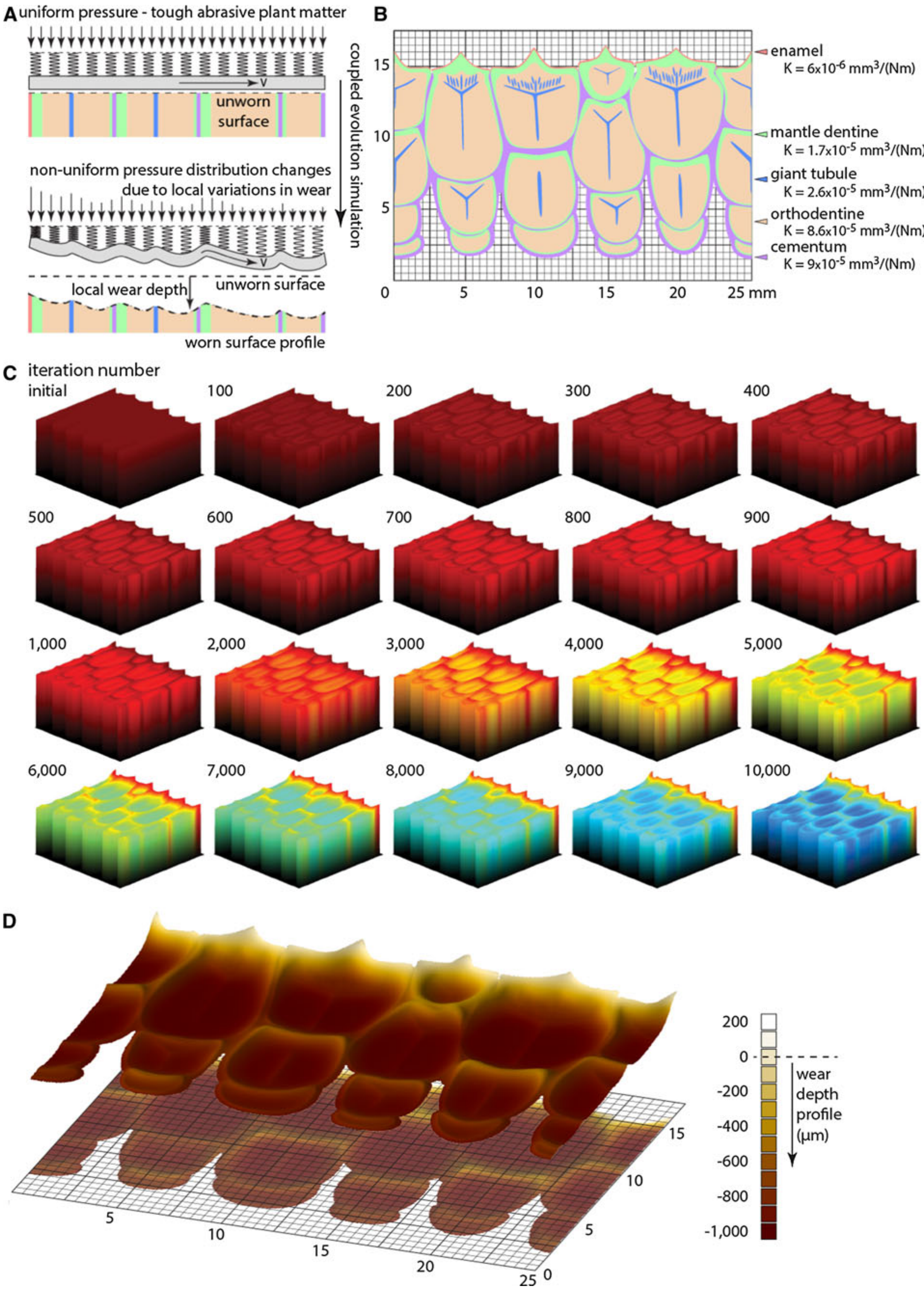

A
uniform pressure - tough abrasive plant matter
v
unworn surface
coupled evolution simulation
non-uniform pressure distribution changes due to local variations in wear
v
local wear depth
unworn surface
worn surface profile
B
enamel
K = 6x10-6 mm3/(Nm)
mantle dentine
K = 1.7x10-5 mm3/(Nm)
giant tubule
K = 2.6x10-5 mm3/(Nm)
orthodentine
K = 8.6x10-5 mm3/(Nm)
cementum
K = 9x10-5 mm3/(Nm)
0
5
10
15
20
25 mm
C
iteration number
initial
100
200
300
400
500
600
700
800
900
1,000
2,000
3,000
4,000
5,000
6,000
7,000
8,000
9,000
10,000
D
200
0
-200
-400
-600
-800
-1,000
wear depth profile (μm)

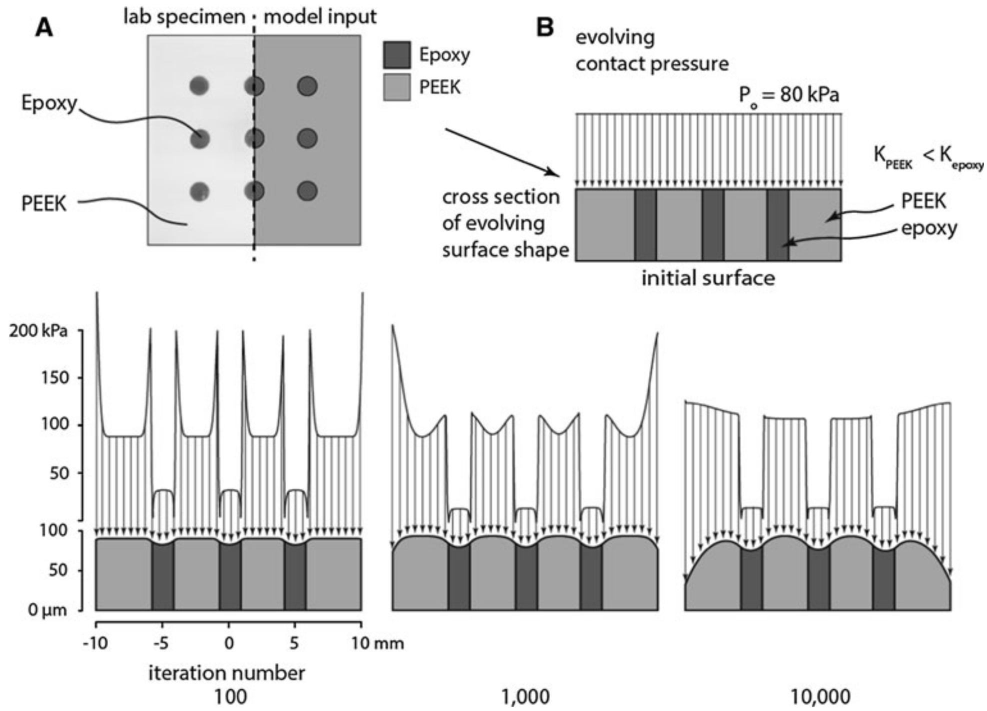

Fig. 2 **a** A model polymer composite for comparing experiments to modeling of the coupled evolution between contact pressure and worn-surface topography. The laboratory sample (*left half*) and the simulation input (*right half*) were compared to illustrate the ability of the simulation to predict worn-surface morphology. **b** Wear and pressure evolution of the model polymeric composite over 10,000 iterations (500 sliding cycles) where an initially uniform pressure distribution evolves with the wearing surface to reach a steady state

fossilized bison tissues revealed that the wear properties of the tissues relative to one another are preserved [16].

Remarkably, the two-parameter elastic foundation contact pressure-coupled wear model demonstrates how the arrangement of the various tissues (Fig. 1b) contribute to producing unique and complex grinding, slicing, cutting, and chewing features (Fig. 1d). This revealed how the individual tissues contribute to whole-tooth wear. The plant fodder was presumed to be a compliant abrasive mat of tough plants with abrasive siliceous phytoliths and other exogenous grit that is approximated in the simulation by this two-parameter foundation model. The simulation begins with a planar surface and runs until the geometry reaches an equilibrium state where the combination of contact pressure, which are higher at prominences, and wear rate results in all components of the system wearing at an equal rate (Fig. 1c). While the actual biological systems are three-dimensional distributions of the tissues within a tooth that is shedding every 45–80 days [19], the two-dimensional model was able to explore how tissue distributions and wear properties act to create self-maintaining surface features through gradual wear (Fig. 1c); the resultant functional shape (Fig. 1d) is a function of dental material area, tissue spacing, and wear rate (e.g., larger expanses of high-wear material produce deeper basins).

3 Model Samples of Polymeric Composite

Now, we transition to an idealized laboratory system to compare the model with a system that can be easily made and measured in the laboratory. A two-component surface comprised of polyetheretherketone (PEEK) and an epoxy resin was used to illustrate the prediction of wear evolution. The surface consisted of a 22.4 × 22.4 mm PEEK square with a 3 × 3 inset array of epoxy circles (Fig. 2a). Each circle was 2 mm in diameter resulting in an area fraction of PEEK and epoxy of ~94 and 6 %, respectively. The PEEK base was machined out of an unfilled bulk material (Quadrant Ketron PEEK). Holes were then drilled and subsequently filled with a two-part epoxy resin and cured under vacuum for 24 h. The test specimen was then machined to be initially flat with a milled surfaced finish and an average roughness of (Ra) ~2 µm. In addition to the composite surface, two additional samples consisting either entirely of PEEK or epoxy were created for the determination of individual abrasive wear rates.

For the abrasive counter sample, a layered system consisting of a 6 mm thick polydimethylsiloxane (PDMS) base with a silicon carbide abrasive paper was used. The abrasive paper was adhered to the top of the PDMS pad and both were clamped to the testing instrument. A 10:1 ratio of elastomer to cross-linker was used to make the Sylgard® 184 PDMS pad, resulting in an elastic modulus of ~1.8 MPa. The silicon carbide abrasive had an average surface roughness (Ra) of ~9.7 µm and a root mean square (RMS) roughness of ~12 µm as determined by an optical profilometer. The first and second foundation parameters for the abrasive PDMS pad used in both the experiment and wear model were measured to be k_s of 0.307 N/mm^3 and k_g of 2.8 N/mm.

4 Experimental Methods: The Coupled Evolution Between Surface Shape and Contact Pressure Wear of a Multicomponent Polymer Composite System

4.1 Tribometer

Wear experiments were performed on a linear reciprocating tribometer [20]. The model polymer composite specimen was mounted to a 6-channel load cell. Opposite the polymer composites was a compliant abrasive pad system comprised of a 400 grit abrasive paper covering a PDMS pad (~6 mm thick); the abrasive pad was mounted directly to a linear ball-screw stage. The composite pin was loaded against the pad to a nominal contact pressure of 80 kPa (~40 N normal load). A prescribed linear sliding stroke of 50.8 mm and a sliding velocity of 50.8 mm/s were used for all experiments. The sample was unloaded, and the abrasive paper was changed after every ten cycles of sliding to reduce the amount of wear debris entrained in the contact until the desired number of cycles were completed. Parameters were selected to create measurable wear in each sub-experiment to allow for rapid comparison with the model.

4.2 Surface Evolution Experiments

The worn-surface profile of the two-component surface sample was periodically monitored. After every 100th sliding cycle, the sample was removed from the tribometer and the resulting worn surface was measured using a Veeco Dektak 8® stylus profilometer. A surface height map was created by stitching numerous individual line scans together, providing height information for a centrally aligned 20 × 20 mm area of the composite surface. The sample was then tested for an additional 100 cycles. This process was repeated until the long wavelength peak to valley heights from the measured surface profiles between 100 cycle increments were within 5 % of each other.

4.3 Wear Rate Measurement of Constituent Materials

Wear rates for constituent materials were measured using the same loading and sliding conditions as the composite sample. The mass of each sample (PEEK or epoxy) was taken before and after each cycle subset during wear rate experiments. The sample was removed every 10 cycles and weighed on a Mettler Toledo scale with a 10 µg precision for wear rate calculations. Using the change in mass [m_{lost} (mm)] and the density of the material [ρ (mg/mm^3)], a wear volume [V_{lost} (mm^3)] was calculated. Wear rates [K (mm^3/Nm)] were calculated by dividing the volume lost during sliding by the normal force [F_N (N)] times the sliding distance [d (m)], (Eq. 4). Wear rates were computed over a total of 50 sliding cycles.

$$K = \frac{V_{\text{lost}}}{F_{\text{N}} d} = \frac{m_{\text{lost}}}{\rho F_{\text{N}} d} \tag{4}$$

5 Results

5.1 Steady State Abrasive Wear Rates

All three samples exhibited a linear relationship between the measured volume loss and the product of applied load and sliding distance at steady state. The wear rates of PEEK and epoxy differed by one order of magnitude while the two-component system (PEEK and epoxy) had a wear rate only slightly higher than that of the purely PEEK sample. Steady state abrasive wear rate values are given in Table 1.

5.2 Model Results

Using the above measured parameters for material wear rates and foundation constants, the wear evolution model was run to simulate 500 cycles of sliding using 10,000 iterations. The pressure and wear evolution of a cross section taken along the middle of the sample is shown in Fig. 2 for various cycle increments. The per-cycle change in volume loss asymptotically approached a steady value around 10,000 iterations. During the early stages of wear, there was a greater volume loss of epoxy material leading to a dishing effect around each of the nine epoxy filled holes (Fig. 3a). Once a steady state was reached, there was a uniform recession of material from both epoxy and PEEK. The edges of the model also showed the development of curvature on the periphery of the sample due to edge effects.

5.3 Wear Evolution of Two-Component Surface

The two-component surface slid a total distance of 50.8 m (500 reciprocating cycles). Surface scans taken upon

Table 1 Steady state abrasive wear rate values for a nominal contact pressure of 80 kPa and 50.8 mm/s sliding velocity

Material	Wear Rate, K (mm^3/Nm)	u (K) (mm^3/Nm)
Epoxy (measured)	2.24×10^{-1}	8.94×10^{-4}
PEEK (measured)	1.98×10^{-2}	1.26×10^{-4}
Composite (measured)	2.12×10^{-2}	1.20×10^{-4}
Composite (Eq. 7 prediction)	2.09×10^{-2}	8.10×10^{-4}
Composite (linear rules of mixture)	3.10×10^{-2}	7.40×10^{-2}

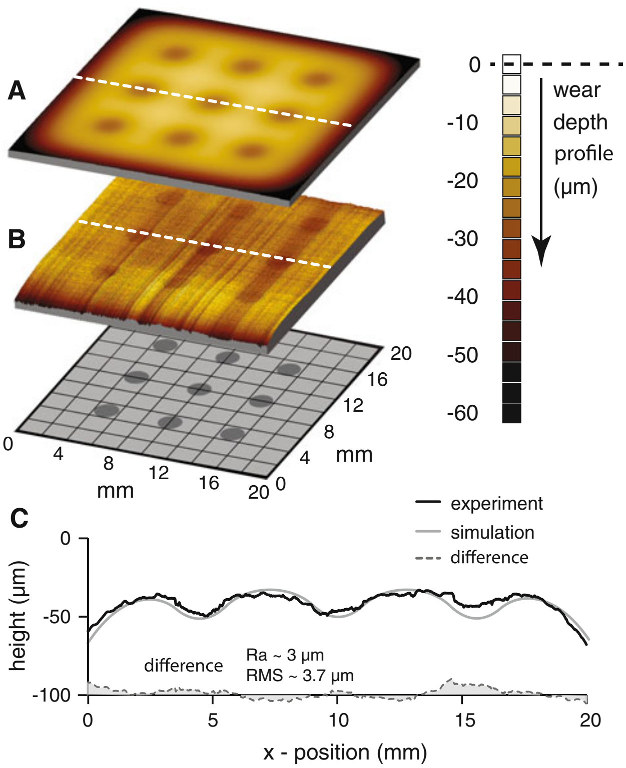

Fig. 3 Steady state two-component system (**a**) model results, (**b**) worn laboratory specimen, and (**c**) line scan comparison between simulation and laboratory results. The difference between the predicted and actual surface shape was on the same order as the specimen's initial surface roughness (~3 μm Ra)

reaching steady state showed pronounced dishing around the epoxy circles and the development of curvature at the sample edges (Fig. 3b). Upon reaching steady state, the recession of material became uniform, wearing both PEEK and epoxy equally.

6 Discussion

6.1 Model Predictions

Line scans from the laboratory sample and modeled surface are compared in Fig. 3c. These surface measurements were taken transverse to the sliding direction at the midpoint of each sample (Fig. 3a, b). The average and RMS roughness of the difference between the modeled and actual surface scans were 2.96 and 3.73 μm, respectively. The differences between the two profiles are probably due to any, or a combination of the following: the accumulation of wear debris within the contact; effects from unidirectional sliding, such as aligned ridges and valleys or dynamic pad reactions. None of these are accounted for within the model. Large curvatures (long wavelengths) compared favorably to modeled data while local changes (short wavelengths) tended to deviate from predictions.

Due to the development of local contact pressures, analytical predictions of the transient wear behavior of the sample are difficult, if not impossible. Using this numerical model and accounting for the local evolution of pressure, an estimate of the run-in behavior of the sample may be made despite complex geometries and material combinations. The ability of the model to accurately predict the evolution of wear and pressure from an initially planar surface depends on the accuracy of the measurement of system parameters; with the pad deflection and bending having a prominent effect on model predictions. It is also important to note that although the model can account for dimensional changes, it does not account for the unidirectional nature of sliding or surface roughness. This can lead to the over or under prediction of wear.

6.2 Combined Wear Rates

The composite surface started as an initially flat surface under a uniform pressure. During sliding, it gradually transformed through a transition phase in which the non-uniform local contact pressures are a function of height and curvature of the surface, resulting in uneven wear of the sample. After the transition phase, the sample reaches a steady state wear regime in which each material recedes the same Δh at each time step. Considering this two-component system with wear rate of $K_{\mathrm{Composite}}$ and average contact pressure $P_{\mathrm{Composite}}$ with one material having a wear rate of K_1 and local contact pressure P_1 and a second material having a wear rate of K_2 and local contact pressure P_2, steady state occurs when:

$$\Delta h \propto K_1 P_1 = K_2 P_2 = K_{\mathrm{Composite}} P_{\mathrm{Composite}} \quad (5)$$

This is only possible if the local contact pressures for a material of given wear rate is constant at all locations of that material in the composite. We can then use a force balance over the constituent materials (Eq. 6) with Eq. 5 to solve for the wear rate of the composite (Eq. 7):

$$P_{\mathrm{Composite}} A_{\mathrm{Composite}} = A_1 P_1 + A_2 P_2 \quad (6)$$

$$K_{\mathrm{Composite}} = \frac{K_1}{A_1^* + A_2^* \left(\frac{K_1}{K_2}\right)} \quad (7)$$

Where A is the area of the material at the surface and A^* is the fractional area (component area divided by total area). The steady state abrasive wear rate of the two-component surface is 2.12×10^{-2} mm^3/(Nm). This is very close to the wear rate predicted by Eq. 7 (2.09×10^{-2} mm^3/(Nm)) and lies between the wear rate of its constituents of PEEK (1.98×10^{-2} mm^3/(Nm)) and Epoxy (2.24×10^{-1} mm^3/(Nm)) (Table 1) and was not predicted by a linear rule of mixtures (3.10×10^{-2} mm^3/(Nm)) [21].

6.3 Applications

The tribological implications of predicting the wear evolution of a multicomponent surface are vast. It is conceivable that these findings may be applied to optimize the wear of 2-D surfaces or to create 3-D surface textures using initially flat surfaces. Potential biologically inspired extensions would be to design self-maintaining surfaces such as the dental battery of the hadrosaurid. Further, biological uses include applications to other taxa (both fossil and extant) with occluding dentitions to gain a better understanding form, function, and performance. However, engineering applications in the design of surfaces remains the most relevant possible use for such a model.

7 Conclusions

The evolution of surface shape and contact pressure for the wear of initially flat surfaces comprised of multiple materials with distinct wear rates was estimated using a two-parameter elastic foundation model. Wear rates measured from fossilized dental tissues were used to elucidate the chewing surface morphology of the hadrosaurid dinosaur. The arrangement of these tissues created a self-maintaining grinding surface, the result of gradual wear from chewing tough plant matter mixed with exogenous abrasive grit.

Experimental abrasive wear experiments obtained of a laboratory multicomponent polymer sample was compared to the model's prediction using the measured system's material parameters (e.g., abrasive wear rates and elastic foundation parameters) as inputs. The differences between the modeled and measured surface profiles were on the same order as the sample's initial surface roughness (Ra $\sim$3 μm). Numerical simulations showed the transient wear behavior and pressure evolution of these multicomponent surfaces; the results of which can be extended to analyze worn surfaces, be used to better understand the development of surface features, or be applied to the design of new components and tribosystems.

Acknowledgments The authors would like to thank the collaborators at the University of Florida Tribology Laboratory for their thoughtful comments and insight as well as Matthew Hamilton, Gerald R. Bourne, Mark A. Norell, and Erica Lilleodden for their contributions to the preliminary hadrosaurid work and NSF (Grant EAR 0959029 and EAR 1226730 to G.M.E.).

References

1. Blanchet, T.: The interaction of wear and dynamics of a simple mechanism. J. Tribol. **119**, 597–599 (1997)
2. Sawyer, W.G.: Wear predictions for a simple-cam including the coupled evolution of wear and load (c). Lubr. Eng. **57**, 31–36 (2001)
3. Dickrell, D.J., Dooner, D.B., Sawyer, W.G.: The evolution of geometry for a wearing circular cam: analytical and computer simulation with comparison to experiment. J. Tribol. **125**, 187–192 (2003)
4. Dickrell, D.J., Sawyer, W.G.: Evolution of wear in a two-dimensional bushing. Tribol. Trans. **47**, 257–262 (2004)
5. Põdra, P., Andersson, S.: Simulating sliding wear with finite element method. Tribol. Int. **32**, 71–81 (1999)
6. Põdra, P., Andersson, S.: Wear simulation with the winkler surface model. Wear **207**, 79–85 (1997)
7. Põdra, P., Andersson, S.: Finite element analysis wears simulation of a conical spinning contact considering surface topography. Wear **224**, 13–21 (1999)
8. Kim, N.H., Won, D., Burris, D., Holtkamp, B., Gessel, G.R., Swanson, P., Sawyer, W.G.: Finite element analysis and experiments of metal/metal wear in oscillatory contacts. Wear **258**, 1787–1793 (2005)
9. Mukras, S., Kim, N.H., Mauntler, N.A., Schmitz, T.L., Sawyer, W.G.: Analysis of planar multi body systems with revolute joint wear. Wear **268**, 643–652 (2010)
10. Mukras, S., Kim, N.H., Sawyer, W.G., Jackson, D.B., Bergquist, L.W.: Numerical integration schemes and parallel computation for wear prediction using finite element method. Wear **266**, 822–831 (2009)
11. Lengiewicz, J., Stupkiewicz, S.: Efficient model of evolution of wear in quasi-steady-state sliding contacts. Wear **303**, 611–621 (2013)
12. Fregly, B.J., Sawyer, W.G., Harman, M.K., Banks, S.A.: Computational wear prediction of a total knee replacement from in vivo kinematics. J. Biomech. **38**, 305–314 (2005)
13. Chongyi, C., Chengguo, W., Ying, J.: Study on numerical method to predict wheel/rail profile evolution due to wear. Wear **269**, 167–173 (2010)
14. Telliskivi, T.: Simulation of wear in a rolling–sliding contact by a semi-winkler model and the Archard's wear law. Wear **256**, 817–831 (2004)
15. Sawyer, W.G.: Surface shape and contact pressure evolution in two component surfaces: application to copper chemical mechanical polishing. Tribol. Lett. **17**, 139–145 (2004)
16. Erickson, G.M., Krick, B.A., Hamilton, M., Bourne, G.R., Norell, M.A., Lilleodden, E., Sawyer, W.G.: Complex dental structure and wear biomechanics in hadrosaurid dinosaurs. Science **338**, 98–101 (2012)
17. Pasternak, P.: On a new method of analysis of an elastic foundation by means of two foundation constants. Gosudarstvennoe Izdatel'stvo Litearturi po Stroitel'stvu i Arkhitekture, Moscow (1954)
18. Timoshenko, S., Woinowsky-Krieger, S., Woinowsky, S.: Theory of plates and shells. McGraw-hill, New York (1959)
19. Erickson, G.M.: Incremental lines of von Ebner in dinosaurs and the assessment of tooth replacement rates using growth line counts. Proc. Natl. Acad. Sci. **93**, 14623–14627 (1996)
20. Schmitz, T.L., Action, J.E., Burris, D.L., Ziegert, J.C., Sawyer, W.G.: Wear-rate uncertainty analysis. J. Tribol. **126**, 802–808 (2004)
21. Gahr, K.: Abrasive wear of two-phase metallic materials with a coarse microstructure. Wear. Mater. **1985**, 45–58 (1985)